Applied Numerical Mathematics 87 (2015) 87–99

Contents lists available at ScienceDirect

Applied Numerical Mathematics

www.elsevier.com/locate/apnum

The Laguerre pseudospectral method for the radial Schrödinger equation

H. Alıcı [a,*], H. Taşeli [b]

[a] Department of Mathematics, Harran University, 63290, Şanlıurfa, Turkey
[b] Department of Mathematics, Middle East Technical University, 06800, Ankara, Turkey

ARTICLE INFO

Article history:
Received 21 April 2014
Received in revised form 5 August 2014
Accepted 3 September 2014
Available online 16 September 2014

Keywords:
Laguerre pseudospectral methods
Radial Schrödinger equation
Quantum mechanical potentials

ABSTRACT

By transforming dependent and independent variables, radial Schrödinger equation is converted into a form resembling the Laguerre differential equation. Therefore, energy eigenvalues and wavefunctions of M-dimensional radial Schrödinger equation with a wide range of isotropic potentials are obtained numerically by using Laguerre pseudospectral methods. Comparison with the results from literature shows that the method is highly competitive.

1. Introduction

In this article, we consider the radial part of the Schrödinger equation in M dimensions

$$\left[-\frac{\mathrm{d}^2}{\mathrm{d}r^2}-\frac{M-1}{r}\frac{\mathrm{d}}{\mathrm{d}r}+\frac{\ell(\ell+M-2)}{r^2}+V(r)\right]\mathcal{R}_{n,\ell}^{(M)}(r)=E_{n,\ell}^{(M)}\mathcal{R}_{n,\ell}^{(M)}(r),\quad \mathcal{R}_{n,\ell}^{(M)}(r)\in L^2(0,\infty) \tag{1}$$

with a variety of quantum mechanical potentials of the form $V(\sqrt{x_1^2+x_2^2+\ldots+x_M^2})=V(r)$, where r denotes the M-dimensional spherical coordinates such that $r^2=\sum_{i=1}^{M}x_i^2$. In (1), $L^2(0,\infty)$ is the Hilbert space of square integrable functions on the half line, $n,\ell=0,1,\ldots$ stand, respectively, for the radial and angular quantum numbers of the energy eigenvalues E and the corresponding wavefunctions $\mathcal{R}(r)$. M-dimensional radial Schrödinger equation has been the subject of many computational methods. The most commonly studied form of (1) is the three-dimensional case with $M=3$

$$\left[-\frac{\mathrm{d}^2}{\mathrm{d}r^2}+\frac{\ell(\ell+1)}{r^2}+V(r)\right]\Psi(r)=\mathcal{E}\Psi(r) \tag{2}$$

in which the first derivative term is removed by making use of the transformation $\Psi(r)=r\mathcal{R}(r)$ on the dependent variable. It is interesting to notice that the last equation can still be derived from (1) without any transformation. To be specific, in (1), regarding M as a parameter with the value $M=1$ and replacing ℓ with $\ell+1$ we obtain (2). Therefore the link between the eigenpairs $\{\mathcal{E}_{n,\ell},\Psi_{n,\ell}(r)\}$ and $\{E_{n,\ell}^{(M)},\mathcal{R}_{n,\ell}^{(M)}(r)\}$ of (2) and (1), respectively, is given by the relations

$$\mathcal{E}_{n,\ell}=E_{n,\ell+1}^{(1)},\qquad \Psi_{n,\ell}(r)=\mathcal{R}_{n,\ell+1}^{(1)}(r). \tag{3}$$

* Corresponding author.
E-mail addresses: haydara@harran.edu.tr (H. Alıcı), taseli@metu.edu.tr (H. Taşeli).

http://dx.doi.org/10.1016/j.apnum.2014.09.001
0168-9274/

Various approximation methods have been proposed for computing the eigenvalues of this problem by many authors. Among them we may recall variational methods [32–34,36,37,39], Hill determinant method [7], pseudospectral methods [2], constant perturbation methods [17,20–22], Prüfer transformation followed by a shooting procedure [4,3], Pekeris-type approximations [12,15,16,18,25,41], asymptotic iteration technique [5] and Hamiltonian hierarchy picture [10].

In particular, in [2], we have studied the Schrödinger equation by an equation of the form

$$\sigma(\xi)y'' + \tau(\xi)y' + Q(\xi)y = -\lambda y, \tag{4}$$

called the equation of hypergeometric type with a perturbation (EHTP), by means of transformations on both independent and dependent variables. Here $\sigma(\xi)$ and $\tau(\xi)$ are polynomials of degrees at most two and one, respectively, and λ is a parameter. In fact, in the special case of $Q(\xi) \equiv 0$, (4) reduces to the well known equation of the hypergeometric type whose suitable solutions are the classical orthogonal polynomials. Accordingly, in [2], we have converted the radial Schrödinger equation in (1) into an EHTP

$$\xi y'' + \left(\ell + \frac{1}{2}M - \xi\right)y' + \frac{1}{4}\left[\xi - c^{-2}V\left(c^{-1}\sqrt{\xi}\right)\right]y = \left(2\ell + M - \frac{1}{4}c^{-2}E\right)y \tag{5}$$

first by introducing the scaled quadratic variable $\xi = (cr)^2$ where c is a positive constant and then proposing a solution of the type $\mathcal{R}(\xi) = \xi^{\ell/2}\mathrm{e}^{-\xi/2}y(\xi)$ satisfying the asymptotic boundary condition at infinity and the regularity condition at the origin. However, the quadratic transformation, which was necessary to convert (1) into an EHTP, does not seem suitable for potentials that contain both odd and even powers of the variable r. For the sake of a form that is well suited for all potentials, we have to sacrifice the EHTP. Therefore, in this study, instead of the quadratic transformation we start with a more flexible one

$$\xi = (cr)^{\alpha}, \quad \alpha, c > 0,\ \xi \in (0, \infty) \tag{6}$$

where the parameters α and c may be exploited to accelerate the convergence rate of the method. Then we suggest a solution of type

$$\mathcal{R}(\xi) = \xi^{\ell/\alpha}\mathrm{e}^{-\xi/2}y(\xi) \tag{7}$$

which transforms the radial Schrödinger equation (1) into

$$\xi y'' + (\gamma + 1 - \xi)y' + Q(\xi)y = \lambda\xi^{\frac{2}{\alpha}-1}y \tag{8}$$

where

$$Q = Q(\xi;\alpha,c,\gamma) = \frac{1}{4}\xi - \frac{1}{2}(\gamma+1) - \frac{1}{(\alpha c)^2}\xi^{\frac{2}{\alpha}-1}V\left(\xi^{1/\alpha}/c\right) \tag{9}$$

represents the modified potential, γ is the parameter

$$\gamma = \gamma(\alpha,\ell,M) = \frac{1}{\alpha}(2\ell + M - 2), \tag{10}$$

and

$$\lambda = \lambda_n(\alpha,c,\gamma) = -\frac{1}{(\alpha c)^2}E^{(M)}_{n,\ell} \tag{11}$$

the rescaled energy eigenvalues.

The positive nonconstant term $\xi^{\frac{2}{\alpha}-1}$ on the right hand side of (8) can be seen as a weight function, and hence, the new form may be considered as a weighted and perturbed Laguerre (WPL) equation. Now the EHTP in (5) is a special case of (8) with $\alpha = 2$. Both (5) and (8) resemble the Laguerre differential equation

$$\xi y'' + (\gamma + 1 - \xi)y' = -ny, \quad \xi \in (0,\infty) \tag{12}$$

where γ is a real parameter and n a non-negative integer. In the next section, we construct the pseudospectral formulation of the WPL equation based on the associated Laguerre polynomials $L_n^{\gamma}(\xi)$ which are the polynomial solutions of (12). Section 3 introduces the numerical examples. Section 4 concerns with the implementation notes and the last section concludes the paper with some remarks.

2. The Laguerre pseudospectral method (LPM) for the WPL equation

A pseudospectral method, also known as spectral collocation method, is based on the N-th degree polynomial interpolation of a function $y(\xi)$ denoted by $P_N(\xi)$,

$$P_N(\xi)=\sum_{n=0}^{N}\ell_n(\xi)y_n, \tag{13}$$

where the $y_n=y(\xi_n)$ are the actual values of $y(\xi)$ at the specified nodes $\xi=\xi_n$ for $n=0,1,\ldots,N$ [6,9,38]. Such a pseudospectral scheme in which the N-th degree Lagrange polynomials

$$\ell_n(\xi)=\frac{\psi_{N+1}(\xi)}{(\xi-\xi_n)\psi'_{N+1}(\xi_n)}=\frac{L^{\gamma}_{N+1}(\xi)}{(\xi-\xi_n)[\frac{\mathrm{d}}{\mathrm{d}\xi}L^{\gamma}_{N+1}(\xi)]_{\xi=\xi_n}},\quad n=0,1,\ldots,N \tag{14}$$

are defined by the normalized

$$\psi_n(\xi)=\frac{1}{h_n}L^{\gamma}_n(\xi),\quad h_n=\sqrt{\frac{\Gamma(n+\gamma+1)}{n!}},\ \gamma>-1 \tag{15}$$

or standard Laguerre polynomials $L^{\gamma}_n(\xi)$ is called a LPM, where the nodes ξ_n are the real, distinct and positive roots of $L^{\gamma}_{N+1}(\xi)$. Approximating the solutions of differential equations by Laguerre polynomials are usually not stable for large N due to their wild behaviors at infinity, and hence, one usually works with the Laguerre functions $\psi_n(\xi)=e^{-\xi/2}L^{\gamma}_n(\xi)/h_n$ instead. This situation is theoretically investigated, for example in [11,24,28,29], and it is shown that the Laguerre functions have better stability properties than Laguerre polynomials. On the other hand, it is stated in [29] on p. 214 that the generalized Laguerre polynomials are useful for the approximation of functions which decay at infinity. Therefore, in this study, we continue with the normalized Laguerre polynomials in (15) since we search for the square integrable solutions of (1) which behave suitably at the origin and vanish exponentially at infinity.

Notice that, $y(\xi_n)=P_N(\xi_n)$ at least at the nodes since the Lagrange polynomials have the well-known property $\ell_n(\xi_m)=\delta_{mn}$ where δ_{mn} is Kronecker's delta. In this article, the discretization procedure of (1) by the LPM for any arbitrary γ parameter is presented keeping in mind that we will eventually take γ as the parameter in (10).

It is also possible to approximate the derivatives of the function $y(\xi)$ by differentiating the interpolant $P_N(\xi)$. Furthermore, the derivative values at the nodes ξ_n may be determined in terms of function values $y_n=P_N(\xi_n)$ by means of a *differentiation matrix* defined by

$$\boldsymbol{D}^{(k)}:=\left[d^{(k)}_{mn}\right]=\frac{\mathrm{d}^k}{\mathrm{d}\xi^k}\left[\ell_n(\xi)\right]\big|_{\xi=\xi_m},\quad k=1,2,\ldots,N \tag{16}$$

for $m,n=0,1,\ldots,N$. The approximate derivative values $\boldsymbol{y}^{(k)}=[P^{(k)}_N(\xi_0),P^{(k)}_N(\xi_1),\ldots,P^{(k)}_N(\xi_N)]^T$ may therefore be written in matrix–vector form

$$\boldsymbol{y}^{(k)}=\boldsymbol{D}^{(k)}\boldsymbol{y} \tag{17}$$

where $\boldsymbol{y}=[y_0,y_1,\ldots,y_N]^T$ is the vector of function values at the nodes. In particular, the entries of the first and the second order differentiation matrices can be obtained as

$$d^{(1)}_{mn}=\frac{1}{2}\begin{cases}\frac{2}{\xi_m-\xi_n}\frac{\psi'_{N+1}(\xi_m)}{\psi'_{N+1}(\xi_n)} & \text{if } m\neq n\\ \frac{1}{\xi_n}(\xi_n-\gamma-1) & \text{if } m=n\end{cases} \tag{18}$$

and

$$d^{(2)}_{mn}=\frac{1}{3}\begin{cases}\frac{3}{\xi_m-\xi_n}[\frac{1}{\xi_m}(\xi_m-\gamma-1)-\frac{2}{\xi_m-\xi_n}]\frac{\psi'_{N+1}(\xi_m)}{\psi'_{N+1}(\xi_n)} & \text{if } m\neq n\\ \frac{1}{\xi_n}[\frac{1}{\xi_n}(\xi_n-\gamma-1)(\xi_n-\gamma-2)-N] & \text{if } m=n\end{cases} \tag{19}$$

by making use of (14) and (16) [35].

On the other hand, the three-term recursion [35]

$$\sqrt{n(n+\gamma)}\psi_{n-1}(\xi)-(2n+\gamma+1-\xi)\psi_n(\xi)-\sqrt{(n+1)(n+\gamma+1)}\psi_{n+1}(\xi)=0 \tag{20}$$

for the normalized Laguerre polynomials may be used to determine the zeros of $\psi_n(\xi)$ and therefore those of $L^{\gamma}_n(\xi)$. Actually, running the above recursion over the range $n=0,1,\ldots,N$ we obtain an inhomogeneous linear algebraic system $(\boldsymbol{W}-\xi\boldsymbol{I})\boldsymbol{t}=\boldsymbol{b}$, or in matrix-vector form

$$\begin{bmatrix} \gamma+1-\xi & -\sqrt{\gamma+1} & 0 & \cdots & 0 \\ -\sqrt{\gamma+1} & \gamma+3-\xi & -\sqrt{2(\gamma+2)} & \ddots & \vdots \\ 0 & -\sqrt{2(\gamma+2)} & \ddots & \ddots & 0 \\ \vdots & \ddots & \ddots & \gamma+2N-1-\xi & -\sqrt{N(\gamma+N)} \\ 0 & \cdots & 0 & -\sqrt{N(\gamma+N)} & \gamma+2N+1-\xi \end{bmatrix} \begin{bmatrix} \psi_0 \\ \psi_1 \\ \vdots \\ \vdots \\ \psi_{N-1} \\ \psi_N \end{bmatrix} = \begin{bmatrix} 0 \\ 0 \\ \vdots \\ \vdots \\ 0 \\ b_{N+1} \end{bmatrix} \tag{21}$$

where $\psi_i = \psi_i(\xi)$ and the right-hand side is a vector with only one nonzero component $b_{N+1} = \sqrt{(N+1)(N+\gamma+1)}\psi_{N+1}(\xi)$. Therefore, if we require $\psi_{N+1}(\xi) = 0$ or, equivalently, $L_{N+1}^{\gamma}(\xi) = 0$ then the system reduces to a standard eigenvalue problem $\boldsymbol{W}\boldsymbol{t} = \xi\boldsymbol{t}$ with the eigenvalue parameter ξ, which provides us the roots ξ_i, $i = 0, 1, \ldots, N$ of $L_{N+1}^{\gamma}(\xi)$ as required [2,35].

Since the eigenvector associated to each eigenvalue of $\boldsymbol{W}$ is unique up to a constant factor, the m-th computed eigenvector

$$\boldsymbol{v}_m = [v_{0,m}, v_{1,m}, \ldots, v_{N-1,m}, v_{N,m}]^T \tag{22}$$

of the matrix $\boldsymbol{W}$ associated to the eigenvalue ξ_m is a constant multiple of $\boldsymbol{t}_m = [\psi_0(\xi_m), \psi_1(\xi_m), \ldots, \psi_{N-1}(\xi_m), \psi_N(\xi_m)]^T$, that is $\boldsymbol{v}_m = a\boldsymbol{t}_m$. The value of a can be determined by considering the first entries $v_{0,m}$ and $\psi_0(\xi_m)$ of the eigenvectors $\boldsymbol{v}_m$ and $\boldsymbol{t}_m$, respectively, since $\psi_0(\xi) = 1/h_0 = 1/\sqrt{\Gamma(\gamma+1)}$ is a constant polynomial we obtain $a = \sqrt{\Gamma(\gamma+1)}v_{0,m}$.

Therefore, for $n = 0, 1, \ldots, N$, the values $\psi_n(\xi_m)$ of the orthonormal Laguerre polynomials at the zeros of $\psi_{N+1}(\xi)$ may be computed as

$$\begin{bmatrix} \psi_0(\xi_m) \\ \psi_1(\xi_m) \\ \vdots \\ \psi_{N-1}(\xi_m) \\ \psi_N(\xi_m) \end{bmatrix} = \frac{1}{\sqrt{\Gamma(\gamma+1)}v_{0,m}} \begin{bmatrix} v_{0,m} \\ v_{1,m} \\ \vdots \\ v_{N-1,m} \\ v_{N,m} \end{bmatrix} \tag{23}$$

in terms of the computed eigenvector $\boldsymbol{v}_m$ of tridiagonal symmetric matrix $\boldsymbol{W}$.

Then we put the interpolant (13) into (8)

$$\sum_{n=0}^{N}\left[\xi\ell_n''(\xi) + (\gamma+1-\xi)\ell_n'(\xi) + Q(\xi)\ell_n(\xi)\right]y_n = \lambda\sum_{n=0}^{N}\xi^{\frac{2}{\alpha}-1}\ell_n(\xi)y_n \tag{24}$$

and demand its satisfaction at the grid points ξ_m for $m = 0, 1, \ldots, N$, to get the discrete representation

$$\boldsymbol{\mathcal{A}}\boldsymbol{y} = \lambda\boldsymbol{\mathcal{B}}\boldsymbol{y} \tag{25}$$

of the WPL. The general entries $\mathcal{A}_{mn}$ and $\mathcal{B}_{mn}$ of the resulting matrices $\boldsymbol{\mathcal{A}}$ and $\boldsymbol{\mathcal{B}}$ are given by

$$\mathcal{A}_{mn} = \xi_m d_{mn}^{(2)} + (\gamma+1-\xi_m)d_{mn}^{(1)} + Q(\xi_m;\alpha,c,\gamma)\delta_{mn} \tag{26}$$

and

$$\mathcal{B}_{mn} = \xi_m^{\frac{2}{\alpha}-1}\delta_{mn} \tag{27}$$

respectively. Since $\boldsymbol{\mathcal{B}}$ is a diagonal matrix, the generalized matrix–eigenvalue problem in (25) can be replaced with the standard one

$$\widehat{\boldsymbol{\mathcal{T}}}\boldsymbol{y} = \lambda\boldsymbol{y} \tag{28}$$

where $\widehat{\boldsymbol{\mathcal{T}}} = \boldsymbol{\mathcal{B}}^{-1}\boldsymbol{\mathcal{A}}$ and its general entry reads as

$$\widehat{\mathcal{T}}_{mn} = \xi_m^{1-\frac{2}{\alpha}}\left[\xi_m d_{mn}^{(2)} + (\gamma+1-\xi_m)d_{mn}^{(1)} + Q(\xi_m;\alpha,c,\gamma)\delta_{mn}\right] \tag{29}$$

where $m, n = 0, 1, \ldots, N$. Here, the vector $\boldsymbol{y}_n = [y_{0,n}, y_{1,n}, \ldots, y_{N,n}]^T$ involves the values of the n-th eigenfunction of (8) associated with the eigenvalue λ_n at the nodal points.

By using (18) and (19) the first two terms in (29) can be incorporated to define

$$\widehat{\mathcal{K}}_{mn} = -\frac{1}{6}\begin{cases} \frac{12\xi_m^{2-\frac{2}{\alpha}}}{(\xi_m-\xi_n)^2}\frac{\psi'_{N+1}(\xi_m)}{\psi'_{N+1}(\xi_n)} & \text{if } m \neq n \\ \xi_n^{1-\frac{2}{\alpha}}\{2N + \frac{1}{\xi_n}[(\gamma-\xi_n)^2 - 1]\} & \text{if } m = n \end{cases} \tag{30}$$

which represents the effect of kinetic energy terms independent of a specified potential.

It seems that the evaluation of $\widehat{\mathcal{K}}_{mn}$ requires the computation of the derivatives $\psi'_{N+1}(\xi_n)$ of the normalized Laguerre polynomials at the nodes. Fortunately, a nice similarity transformation $\boldsymbol{\mathcal{T}} = \boldsymbol{S}^{-1}\widehat{\boldsymbol{\mathcal{T}}}\boldsymbol{S}$ in which

$$\boldsymbol{S} = s_m\delta_{mn} = \xi_m^{1-\frac{1}{\alpha}}\psi'_{N+1}(\xi_m)\delta_{mn} \tag{31}$$

is a diagonal matrix, makes it possible to get rid of such a cumbersome labor. Furthermore, the matrix in (28) reduces to a symmetric one, say $\boldsymbol{\mathcal{T}} = \boldsymbol{S}^{-1}(\widehat{\boldsymbol{\mathcal{K}}} + \boldsymbol{\mathcal{Q}})\boldsymbol{S}$, whose entries are given by

$$\mathcal{T}_{mn} = \mathcal{K}_{mn} + \mathcal{Q}_{mn} \tag{32}$$

where

$$\mathcal{K}_{mn} = -\frac{1}{6}\begin{cases} \frac{12(\xi_m\xi_n)^{1-\frac{1}{\alpha}}}{(\xi_m-\xi_n)^2} & \text{if } m \neq n \\ \xi_n^{1-\frac{2}{\alpha}}\{2N + \frac{1}{\xi_n}[(\gamma-\xi_n)^2 - 1]\} & \text{if } m = n \end{cases} \tag{33}$$

and

$$\mathcal{Q}_{mn} = \xi_m^{1-\frac{2}{\alpha}}Q(\xi_m;\alpha,c,\gamma)\delta_{mn} = \xi_m^{1-\frac{2}{\alpha}}\left[\frac{1}{4}\xi_m - \frac{1}{2}(\gamma+1) - \frac{1}{(\alpha c)^2}\xi_m^{\frac{2}{\alpha}-1}V\left(\xi_m^{1/\alpha}/c\right)\right]\delta_{mn}. \tag{34}$$

Thus, the eigenvalues of (28), and, hence, the approximate eigenvalues of the WPL can be determined by the symmetric matrix eigenvalue problem

$$\boldsymbol{\mathcal{T}}\boldsymbol{u} = \lambda\boldsymbol{u} \tag{35}$$

since the similar matrices share the same spectrum. Note that, the Laguerre pseudospectral formulation of the WPL leads to the symmetric matrix eigenvalue problem whose construction requires only the knowledge of the roots of the Laguerre polynomial $L_{N+1}^{\gamma}(\xi)$.

On the other hand, the n-th eigenvector $\boldsymbol{y}_n$ of (28) is given by the formula

$$\boldsymbol{y}_n = \boldsymbol{S}\boldsymbol{u}_n \tag{36}$$

in terms of the n-th eigenvector $\boldsymbol{u}_n = [u_{0,n}, u_{1,n}, \ldots, u_{N,n}]^T$ of the symmetric matrix $\boldsymbol{\mathcal{T}} = \boldsymbol{S}^{-1}\widehat{\boldsymbol{\mathcal{T}}}\boldsymbol{S}$ since $\boldsymbol{S}^{-1}\widehat{\boldsymbol{\mathcal{T}}}\boldsymbol{S}\boldsymbol{u} = \lambda\boldsymbol{u}$ implies that $\widehat{\boldsymbol{\mathcal{T}}}[\boldsymbol{S}\boldsymbol{u}] = \lambda[\boldsymbol{S}\boldsymbol{u}]$. Thus, the m-th entry $y_{m,n} = y_n(\xi_m)$ of the n-th eigenvector $\boldsymbol{y}_n$ may be written as $y_{m,n} = s_m u_{m,n}$, or in nodal notation we have

$$y_n(\xi_m) = \xi_m^{1-\frac{1}{\alpha}}\psi'_{N+1}(\xi_m)u_{m,n} \tag{37}$$

upon using (31). Then (7) determines the original wavefunction

$$\mathcal{R}_{n,\ell}^{(M)}(\xi_m) = \psi'_{N+1}(\xi_m)\xi_m^{1+\frac{\ell-1}{\alpha}}e^{-\xi_m/2}u_{m,n} \tag{38}$$

at a collocation point ξ_m. Turning back to the original variable r via (6), the last equation reads as

$$\mathcal{R}_{n,\ell}^{(M)}(r_m) = \psi'_{N+1}\left((cr_m)^{\alpha}\right)(cr_m)^{\alpha+\ell-1}e^{-(cr_m)^{\alpha}/2}u_{m,n}. \tag{39}$$

Thus, we may state the following theorem.

Theorem 2.1. *The approximate eigenvalues $E_{n,\ell}^{(M)}$ of the radial Schrödinger equation in (1) are connected with the eigenvalues of the linear system in (35) by the formula*

$$E_{n,\ell}^{(M)} = -(\alpha c)^2\lambda_n(\alpha,c,\gamma), \quad n = 0, 1, \ldots \tag{40}$$

and the values of the corresponding normalized eigenfunctions $\mathfrak{R}_{n,\ell}^{(M)}(r_m)$ (in L_ρ^2 sense) at the points $r_m = \xi_m^{1/\alpha}/c$ are given by

$$\mathfrak{R}_{n,\ell}^{(M)}(r_m) = \sqrt{\alpha c^M}\mathcal{R}_{n,\ell}^{(M)}(r_m) = -\sqrt{\frac{\alpha c^M(N+1)(N+\gamma+1)}{\Gamma(\gamma+1)}}\frac{v_{N,m}}{v_{0,m}}(cr_m)^{\alpha+\ell-1}e^{-(cr_m)^{\alpha}/2}u_{m,n} \tag{41}$$

whenever $\boldsymbol{u}_n$ is the normalized (in Euclidean 2-norm) eigenvector of (35). The $v_{0,m}$ and $v_{N,m}$ are the first and the last entries of (22), respectively.

Proof. The first part follows from (11). When written in the Sturm–Liouville form, it is not difficult to see that the weight functions of (1) and (8) are given by $\rho(r)=r^{M-1}$ and $\rho(\xi)=\xi^{\gamma+\frac{2}{\alpha}-1}e^{-\xi}$, respectively. First using the scaling transformation in (6) we write

$$\left\|\Re_{n,\ell}^{(M)}(r)\right\|_{L^2_{\rho(r)}}^2=\int_0^\infty\left[\Re_{n,\ell}^{(M)}(r)\right]^2r^{M-1}\mathrm{d}r=\int_0^\infty\left[\sqrt{\alpha c^M}\mathcal{R}_{n,\ell}^{(M)}(r)\right]^2r^{M-1}\mathrm{d}r=\int_0^\infty\left[\mathcal{R}_{n,\ell}^{(M)}(\xi)\right]^2\xi^{\frac{M}{\alpha}-1}\mathrm{d}\xi \tag{42}$$

which, upon the use of (7), reads as

$$\left\|\Re_{n,\ell}^{(M)}(r)\right\|_{L^2_{\rho(r)}}^2=\int_0^\infty y_n^2(\xi)\xi^{\gamma+\frac{2}{\alpha}-1}e^{-\xi}\mathrm{d}\xi. \tag{43}$$

Applying the $N+1$ point Laguerre–Gauss quadrature to the function $\xi^{\frac{2}{\alpha}-1}y_n^2(\xi)$, we obtain, in the limiting case when $N\to\infty$

$$\left\|\Re_{n,\ell}^{(M)}(r)\right\|_{L^2_{\rho(r)}}^2=\int_0^\infty\xi^{\frac{2}{\alpha}-1}y_n^2(\xi)\xi^{\gamma}e^{-\xi}\mathrm{d}\xi=\lim_{N\to\infty}\sum_{m=0}^{N}\xi_m^{\frac{2}{\alpha}-1}y_n^2(\xi_m)\omega_m \tag{44}$$

where

$$\omega_m=\frac{1}{(N+1)(N+\gamma+1)}\frac{\xi_m}{\psi_N^2(\xi_m)},\quad m=0,1,\ldots,N \tag{45}$$

are known as the Christoffel numbers or weights of the quadrature in terms of the normalized Laguerre polynomials [13]. Now, the differential-difference relation [35]

$$\xi\psi_n'(\xi)=n\psi_n(\xi)-\sqrt{n(n+\gamma)}\psi_{n-1}(\xi) \tag{46}$$

of the normalized Laguerre polynomials with $n=N+1$ and $\xi=\xi_m$ leads to

$$\psi_{N+1}'(\xi_m)=-\frac{1}{\xi_m}\sqrt{(N+1)(N+\gamma+1)}\psi_N(\xi_m) \tag{47}$$

since $\psi_{N+1}(\xi_m)=0$ for $m=0,1,\ldots,N$ and hence, (37) rewritten as

$$y_n(\xi_m)=-\sqrt{(N+1)(N+\gamma+1)}\psi_N(\xi_m)\xi_m^{-\frac{1}{\alpha}}u_{m,n}. \tag{48}$$

Inserting (45) and (48) into the right hand side of (44) we obtain

$$\left\|\Re_{n,\ell}^{(M)}(r)\right\|_{L^2_{\rho(r)}}^2=\lim_{N\to\infty}\sum_{m=0}^{N}u_{m,n}^2=\lim_{N\to\infty}\|\boldsymbol{u}_n\|_2^2=\lim_{N\to\infty}1=1. \tag{49}$$

On the other hand, (39) together with (47) and (23) gives (41) which completes the proof. It is clear from (43) and (49) that

$$\left\|y_n(\xi)\right\|_{L^2_{\rho(\xi)}}=1 \tag{50}$$

is also true under the same assumption where $\rho(\xi)=\xi^{\gamma+\frac{2}{\alpha}-1}e^{-\xi}$. □

3. Numerical examples

It is clear from (8) and (10) that the spectrum of the eigenvalue problem remains unchanged for a prescribed value of the sum $2\ell+M$. Hence the eigenvalues in M dimensions denoted by $E_{n,\ell}^{(M)}$ are degenerate in such a way that

$$\begin{aligned}
&E_{n,1}^{(2)}\equiv E_{n,0}^{(4)}\\
&E_{n,2}^{(2)}\equiv E_{n,1}^{(4)}\equiv E_{n,0}^{(6)}\\
&\vdots\\
&E_{n,\ell}^{(2)}\equiv E_{n,\ell-1}^{(4)}\equiv E_{n,\ell-2}^{(6)}\equiv\ldots\equiv E_{n,2}^{(2\ell-2)}\equiv E_{n,1}^{(2\ell)}\equiv E_{n,0}^{(2\ell+2)}
\end{aligned} \tag{51}$$

Table 1
The energy eigenvalues $E^{(3)}_{n,\ell}$ of the potential, $V(r) = r^2 + v_4 r^4$, as a function of v_4 where $\alpha_{opt} = 2$.

v_4	c_{opt}	N	n	l	$E^{(3)}_{n,\ell}$
10^{-4}	1	8	0	0	3.000 374 896 936 121 098 337 846 829 9
	1	40	25	1	105.410 343 852 439 559 553 621 014 591 0
	1	66	50	5	214.674 964 990 804 822 025 570 511 216 2
	1	124	100	10	429.514 482 011 916 008 399 592 238 938
1	3	30	0	10	54.184 984 610 454 439 924 123 480 175 6[a]
	3	65	25	5	483.022 207 413 394 709 428 608 270 729 1
	2.5	100	50	1	1062.889 853 853 655 671 834 975 735 691
	2	160	100	0	2604.432 485 714 639 307 459 405 681 55
10^4	9	30	0	0	81.903 316 953 284 467 567 471 308 555
	9	80	25	1	9253.923 499 415 499 714 821 586 373 98
	12	100	50	5	23756.533 983 690 976 108 458 514 955 3
	13	162	100	10	59302.060 313 455 515 491 294 154 604 9

[a] Reference [36]: $E^{(3)}_{0,10} = 54.184\,984\,610\,454\,439\,924\,123\,480\,175\,7$.

Table 2
The effect of second optimization parameter α on the accuracy of ground state energies of isotropic quartic oscillator when $v_4 = 10^{-4}$ and the Airy equation.

α	$E^{(3)}_{0,0}$ of isotropic quartic oscillator ($N = 8, c_{opt} = 1$)	$E^{(1)}_{0,1} = \mathcal{E}_{0,0}$ of Airy equation ($N = 66, c_{opt} = 6$)
3	3.066 750	9.111 969
2.5	3.026 398	4.842 756
2	3.000 374 896 936 121 098 337 846 829 9	2.632 534
1.5	2.993 411	2.338 107 893
1	2.946 460	2.338 107 410 459 767 038 489 197 252 4
0.5	3.027 127	2.338 111

for even values of space dimension M where $E^{(2)}_{n,0}$ is single in the system. Similarly, if M is odd, then

$$\begin{aligned}
&E^{(3)}_{n,0} \equiv E^{(1)}_{n,1} \equiv \mathcal{E}_{n,0}\\
&E^{(3)}_{n,1} \equiv E^{(5)}_{n,0}\\
&E^{(3)}_{n,2} \equiv E^{(5)}_{n,1} \equiv E^{(7)}_{n,0}\\
&\vdots\\
&E^{(3)}_{n,\ell} \equiv E^{(5)}_{n,\ell-1} \equiv E^{(7)}_{n,\ell-2} \equiv \ldots \equiv E^{(2\ell-1)}_{n,2} \equiv E^{(2\ell+1)}_{n,1} \equiv E^{(2\ell+3)}_{n,0}
\end{aligned} \tag{52}$$

where $\mathcal{E}_{n,0}$ are the eigenvalues of the Schrödinger equation in (2). The degenerate structure of the spectrum of (1) now suggests evidently that we may consider only two- and three-dimensional cases, without any loss of generality.

As a first example we consider the M-dimensional isotropic quartic oscillator

$$V(r) = r^2 + v_4 r^4 \tag{53}$$

where $v_4 > 0$. Taşeli and Zafer [36] expanded the wave function into a Fourier–Bessel series to solve the radial Schrödinger equation with isotropic polynomial potentials and Taşeli [32] proposed an alternative series solution to the isotropic quartic oscillator in M dimensions. It seems that the transformation (6) with $\alpha = 2$ is the most suitable one since the potential contains even powers of r only. In Table 1, we present eigenvalues of isotropic quartic oscillator in 3-dimensions for some pairs of (n, l). In all tables, n and ℓ stand for the quantum numbers of the state, N the truncation order for which the desired (machine) accuracy of the corresponding eigenvalue is obtained, and c and α denote some scaling or optimization parameters which may be used to accelerate the convergence rate of the method. The accuracy of the results in all tables reported here has been checked by inspecting the number of stable digits between two consecutive truncation orders. For comparison, at the bottom right of Table 1 we included a result from [36] when $v_4 = 1$.

On the other hand, the effect of the second optimization parameter α is reported in Table 2. In order to regain the machine accuracy for $E^{(3)}_{0,0}$ when, for example, $\alpha = 1$ we should choose $N = 50$ and $c = 15$ at the same time. Therefore, we may say that our prediction of α is experimentally justified by Table 2. If further $c = 1$, that is, in the absence of scaling factors, the truncation order N increases dramatically. For unbounded domains scaling factors are crucial to obtain the desired accuracy with the possible smallest truncation order.

The second example is an odd polynomial potential

Table 3
Several eigenvalues of the Airy equation when $\alpha_{opt} = 1$. The last column includes the negatives of first ten zeros of Airy function Ai(x).

c_{opt}	N	n	$\mathcal{E}_{n,0} = E^{(1)}_{n,1}$	Reference [1]
6	66	0	2.338 107 410 459 767 038 489 197 252 4	2.338 107 41
		1	4.087 949 444 130 970 616 636 988 701 4	4.087 949 44
		2	5.520 559 828 095 551 059 129 855 5129	5.520 559 83
		3	6.786 708 090 071 758 998 780 246 384 5	6.786 708 09
		4	7.944 133 587 120 853 123 138 280 555 8	7.944 133 59
		5	9.022 650 853 340 980 380 158 190 839 9	9.022 650 85
		6	10.040 174 341 558 085 930 594 556 737 3	10.040 174 34
		7	11.008 524 303 733 262 893 235 439 6496	11.008 524 30
		8	11.936 015 563 236 262 517 006 364 902 9	11.936 015 56
		9	12.828 776 752 865 757 200 406 729 407 2	12.828 776 75
6	66	10	13.691 489 035 210 717 928 295 696 779 4	
6	70	20	21.224 829 943 642 095 368 459 920 359 3	
8	110	30	27.588 387 809 882 444 811 950 364 414 1	
9	135	40	33.284 884 681 901 401 879 619 739 896 0	
10	155	50	38.528 808 305 094 248 822 629 896 744 7	
15	280	100	60.858 931 764 608 923 795 521 455 753 8	

$$V(r) = r, \quad r \in (0, \infty) \tag{54}$$

for which the Schrödinger equation reduces to the Airy equation $-y'' + ry = \lambda y$ when we set $M = 1$ and $\ell = 0$ or $\ell = 1$ in (1). In this case, eigenvalues are given implicitly by $\mathrm{Ai}(-\lambda) = 0$ where Ai(x) is the Airy function [8]. Several states of the Airy equation in one dimension is reported in Table 3. The last column includes the negatives of zeros of the Airy function taken from [1]. It is clear from Table 2 that for the Airy equation the optimum value of the second scaling factor is $\alpha_{opt} = 1$.

As a third example, we consider the exponential cosine partially screened Coulomb potential (ECPSC)

$$V(r) = -2ZV_{ec}(r, \nu, \mu) - 2Z_{as}\left[\frac{1}{r} - V_{ec}(r, \nu, \mu)\right], \quad Z > 0,\ Z_{as} > 0 \tag{55}$$

where

$$V_{ec}(r, \nu, \mu) = \frac{1}{r}\mathrm{e}^{-\nu r}\cos(\mu r) \tag{56}$$

with the two screening parameters ν and μ [17]. In particular, when $Z_{as} = 0$ the potential reduces to the exponential cosine screened Coulomb potential (ECSC) $V(r) = -2Z\exp(-\nu r)\cos(\mu r)/r$. If further, $\mu = 0$ at the same time, it is known as the Yukawa potential $V(r) = -2Z\exp(-\nu r)/r$. On the other hand, $Z_{\mathrm{as}} = Z$ corresponds to the pure attractive Coulomb potential $V(r) = -2Z/r$ which has countably many discrete states given by

$$E^{(M)}_{n,\ell} = \frac{-4Z^2}{(2n + 2\ell + M - 1)^2}, \quad n = 0, 1, \ldots \tag{57}$$

together with the continuous spectrum over the entire positive real axis.

These potentials have been subject of several studies. For example, Lai [19] determined several states of ECSC within the framework of the hypervirial Padé scheme. Taşeli [33] used modified Laguerre basis for the ECSC and Yukawa potentials. Ixaru and co-workers [17] developed accurate, robust and safe approach for ECPSC.

Several eigenvalues of the ECPSC potential in three dimensions are reported in Table 4 for the parameter values $Z = 50$, $Z_{as} = 1$ and $\nu = \mu = 0.025$ when $\ell = 0, 10$. It is clear from Table 4 that if we keep $\alpha = 1$, higher levels become expensive or even impossible to obtain. In this stage, transformations (6) and (7) together with the decreasing character of c suggests that we should take smaller α values. Indeed, when we take $\alpha = 0.7$ while keeping $c = 1$, it is possible to obtain higher states with relatively small truncation orders.

Table 5 demonstrates the bound states of the ECSC potential. In all computations we used quadruple-precision arithmetic on a main frame computer with machine accuracy of 32 digits, by truncating the results to 27–28 significant figures. For comparison, at the bottom right of the table, we attached results from [33] and [21] which are in good agreement with those of the present study to the accuracy quoted.

Fig. 1 illustrates the two normalized eigenfunctions $\Psi_{30,0}(r)$ and $\Psi_{4,0}(r)$ of the ECPSC and ECSC potentials, respectively, for the specified parameter values. Our results are in good agreement with those of MATSLISE, which is typical for all eigenfunctions considered in this study.

The present method works well also for the pure attractive Coulomb potential. For instance, in three dimensions when $Z_{as} = Z = 1$, $\ell = 0$, $\alpha = 1$ and $N = 500$, the eigenvalues $E^{(3)}_{n,0}$ with $2 \le n \le 125$ are obtained within the machine accuracy by taking $c = 0.05$ while $c = 0.005$ leads to the same accuracy for $E^{(3)}_{n,0}$ with $130 \le n \le 430$. That is, the optimization parameters may be seen as the position identifier of a flash lamp which illuminates the specific part of the eigenvalue

Table 4
Several states of the ECPSC potential in three dimensions when $Z = 50$, $Z_{as} = 1$ and $\nu = \mu = 0.025$ as ℓ varies.

α_{opt}	c_{opt}	N	n	ℓ	$E^{(3)}_{n,\ell} = E^{(1)}_{n,\ell+1} = \mathcal{E}_{n,\ell}$	$\mathcal{E}_{n,\ell}$ (Reference [17])
1	90	20	0	0	−2497.550 000 612 117 302 611 999 477 0	−2497.550 000 612 0
	60	20	1		−622.550 008 558 171 072 433 651 132 85	−622.550 008 557
	30	20	2		−275.327 819 864 885 534 764 663 309 750	−275.327 819 864
	8	30	10		−18.218 254 864 529 448 891 256 063 943 9	−18.218 254 864
	5	40	20		−3.301 293 923 744 987 946 825 007 566 6	Not reported
	3	62	30		−0.477 979 395 108 803 362 523 577 038 9	Not reported
	0.5	325	50		−0.001 531 833 374 319 363 664 975 806 4	−0.001 531 833 374
0.7	1	350	100		−0.000 174 507 058 491 51	−0.000 174 507 058 49
1	8	25	0	10	−18.214 451 240 408 459 529 166 833 611 8	−18.214 451 240 40
	8	25	1		−14.916 599 484 348 635 959 872 635 251 2	−14.916 599 484 3
	8	25	2		−12.351 299 229 508 114 531 034 516 078 1	−12.351 299 229 4
	5	40	10		−3.289 943 284 017 899 997 236 108 480 7	−3.289 943 284 01
	4	80	20		−0.460 117 420 637 774 647 219 316 169 8	Not reported
	0.7	200	30		−0.003 368 086 423 513 184 468 068 809 9	Not reported
	.3	355	50		−0.000 699 631 092 664 645 508	−0.000 699 631
0.7	1	350	100		−0.000 129 394 044 816 757 730	−0.000 129 394 0

Table 5
Bound energy eigenvalues of the ECSC potential in three dimensions when $Z = 1$ and $\nu = 0.05$, as μ varies. The case, $\mu = 0$ corresponds to the Yukawa potential.

μ	c_{opt}	α_{opt}	N	n	ℓ	$E^{(3)}_{n,\ell}$
0	0.6	1	65	0	0	−0.903 632 857 049 011 087 712 434 151 5[a]
				1		−0.163 542 391 590 506 248 346 978 827 5
				2		−0.038 705 109 629 504 684 590 795 993 6
				3		−0.006 183 319 800 322 642 969 317 900 6
	1	0.5	250	4		−0.000 003 138 989 336 707 735 885 268[b]
	0.4	1	56	0	1	−0.161 480 774 075 569 219 424 205 487 2
				1		−0.037 115 503 766 811 993 209 787 987 8
				2		−0.005 196 117 705 143 707 930 522 382 5
	0.4	1	51	0	2	−0.033 831 141 139 631 685 772 229 516 5
				1		−0.003 161 743 253 742 009 905 767 896 1
0.05	1	1	55	0	0	−0.900 234 932 841 375 336 090 552 641 8
				1		−0.152 899 192 500 495 488 768 133 761 7
				2		−0.023 151 128 414 121 591 695 111 322 3
			55	0	1	−0.152 118 024 883 462 094 709 873 149 7
				1		−0.021 858 659 645 112 322 497 129 462 4
			55	0	2	−0.019 109 758 645 475 738 881 842 814 0

[a] Appropriately scaled result from Reference [33]: $E^{(3)}_{0,0} = -0.903\,632\,857\,049\,011\,087\,712\,434$.

[b] MATSLISE [21]: $E^{(3)}_{4,0} = E^{(1)}_{4,1} = \mathcal{E}_{4,0} = -0.000\,003\,138\,989\,337$.

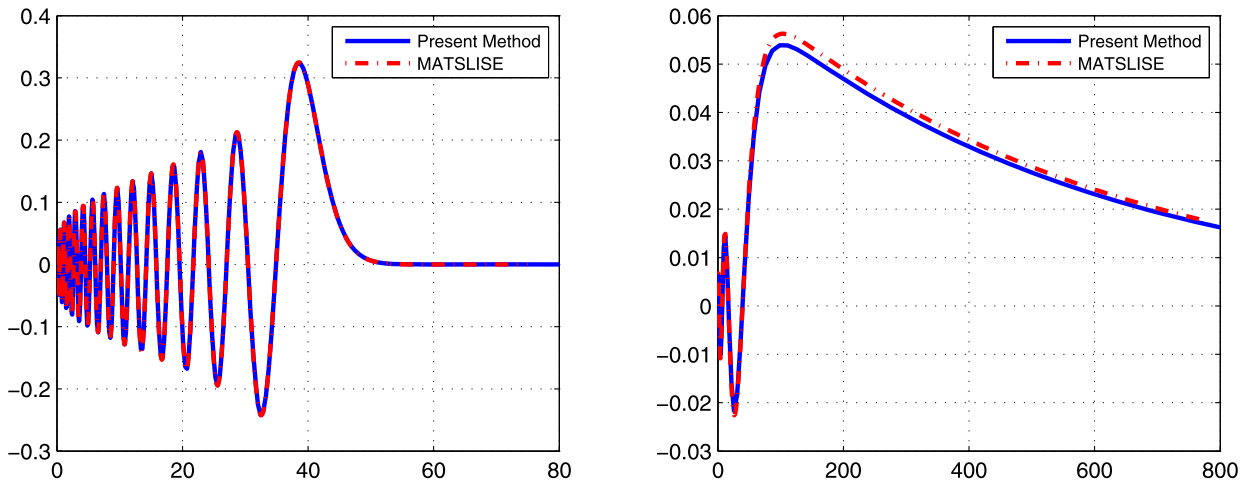

Fig. 1. Normalized eigenfunction $\Psi_{30,0}(r) = \mathcal{R}^{(1)}_{30,1}(r)$ of the ECPSC potential corresponding to $E^{(1)}_{30,1} = \mathcal{E}_{30,0}$ when $Z = 50$, $Z_{as} = 1$, $\nu = \mu = 0.025$ (left). Normalized eigenfunction $\Psi_{4,0}(r) = \mathcal{R}^{(1)}_{4,1}(r)$ of the ECSC potential corresponding to $E^{(1)}_{4,1} = \mathcal{E}_{4,0}$ when $Z = 1$, $\nu = 0.05$, $\mu = 0$ (right).

Table 6
Bound states of the Hulthén screening potential in three dimensions when $Z = 50$ and $\nu = 0.025$, as ℓ varies ($\alpha_{opt} = 1$).

c_{opt}	N	n	ℓ	$E^{(3)}_{n,\ell} = E^{(1)}_{n,\ell+1}$	$\mathcal{E}_{n,\ell}$ (Reference [17])
60	60	0	0	−2498.750 156 250 000 000 000 000 000 000 019 8	
		1		−623.750 625 000 000 000 000 000 000 000 007	
		2		−276.529 184 027 777 777 777 777 777 779 5	
		3		−155.002 500 000 000 000 000 000 000 001 6	
0.5	350	59		−0.006 944 444 444 444 444 444 444 444 4	
		60		−0.003 268 652 579 951 625 907 014 243 5	
		61		−0.000 989 203 954 214 360 041 623 309 1	
		62		−0.000 037 832 262 534 6	
8	30	0	10	−19.424 335 304 526 595 443 026 049 233 6	−19.424 335 304 52
		1		−16.127 883 961 903 674 884 056 154 659 1	−16.127 883 961 9
		2		−13.563 579 616 949 111 137 705 699 537 1	−13.563 579 616 9
		3		−11.530 002 448 250 049 695 932 487 845 2	−11.530 002 448 2
1	250	47		−0.015 675 609 084 845 879 723 414 562 8	Not reported
		48		−0.009 260 969 711 122 159 378 014 469 3	−0.009 260 969 71
		49		−0.04 448 783 837 632 467 073 719 998 2	−0.00 448 783 83
		50		−0.001 188 166 258 891 096 462 375 433 4	−0.001 188 166 259

column. Therefore, adjusting the position of the flashlight, it is possible to lightening the whole set of eigenvalues for a prescribed truncation order N.

The next potential we consider is the partially screening Hulthén potential

$$V(r) = -2ZV_H(r,\nu) - 2Z_{as}\left[\frac{1}{r} - V_H(r,\nu)\right], \quad Z > 0, \quad Z_{as} > 0 \tag{58}$$

where

$$V_H(r,\nu) = \frac{\nu e^{-\nu r}}{1 - e^{-\nu r}} \tag{59}$$

in which ν is the screening parameter. It reduces to the Hulthén screening potential [14] when $Z_{as} = 0$ which is exactly solvable when $M = \ell = 1$ (or $\bar{\ell} = 0$). In this case, bound states are given by

$$E^{(1)}_{n,1} = \mathcal{E}_{n,0} = -\left[\frac{Z}{n+1} - \frac{(n+1)\nu}{2}\right]^2, \quad n = 0, 1, \ldots, k \tag{60}$$

where $k = \lfloor \sqrt{2Z/\nu} \rfloor - 1$ [8]. Here $\lfloor a \rfloor$ denotes the integer part of a real number a.

The partially screening Hulthén potential is considered by Ixaru, De Meyer and Vanden Berghe [17]. Hulthén potential is studied by many authors. For instance, Roy [26] applied the generalized pseudospectral approach to approximate the bound states, Stubbins [30] used the generalized variational method to compute the eigenvalues for $n \leq 6$, Bayrak and Boztosun [5] used asymptotic iteration method for any ℓ state and Gönül and co-workers [10] considered the potential in the Hamiltonian hierarchy picture to approximate the eigenvalues when $\ell \neq 0$.

Table 6 illustrates the bound states of the Hulthén screening potential in three dimensions when $Z = 50$ and $\nu = 0.025$. For $\ell = 0$ the results are in good agreement with the exact eigenvalues. The last column includes results from [17] when $\ell = 10$, which are also in good agreement to the accuracy quoted.

Finally, we take into account the Woods–Saxon potential defined by

$$V(r) = -\frac{50}{1+t}\left[1 - \frac{5t}{3(1+t)}\right] \tag{61}$$

where $t = \exp[3/5(r-7)]$. The potential has been considered by several authors; Zakrzewski [40] used a power series method, Lo and Shizgal [23] applied quadrature discretization method, Shao and Wang [27] considered Obrechkoff one-step method to approximate the eigenvalues of the problem.

Bound states of the Woods–Saxon potential in two dimensions when $\ell = 2$ and in three dimension when $\ell = 0$ are reported in Table 7. In both cases, there exist 14 discrete states before the start of continuous spectrum over the entire positive real axis.

Fig. 2 shows the first eigenfunction $\Psi_{1,0}(r) = \mathcal{R}^{(1)}_{1,1}(r)$ of the Woods–Saxon potential by using $N = 120$ points for different values of the optimization parameter c while keeping $\alpha = 1$. At this truncation order, the optimum c value is $c_{opt} = 45$. Notice that, c_{opt} collects the grid points to the region where the eigenfunction is nonzero. Neither the points are wasted in the region where the wavefunction is too close to zero, nor they are insufficient to recover the shape of the eigenfunction. In this way, it reduces the number N of collocation points used to get the desired accuracy. Here, for $c = 15$ and $c = 45$, the energy $\mathcal{E}_{1,0} = E^{(1)}_{1,1}$ is correct to 20 and 27 digits respectively, but no convergence occurs when $c = 100$ for the same truncation order of $N = 120$.

Table 7
Some bound states $E_{n,\ell}^{(M)}$ of Woods–Saxon potential.

n	$E_{n,2}^{(2)}(N=240,\ c_{opt}=20,\ \alpha_{opt}=1)$	$E_{n,0}^{(3)}=E_{n,1}^{(1)}=\mathcal{E}_{n,0}(N=200,\ c_{opt}=30,\ \alpha_{opt}=1)$
0	−48.661 955 435 951 756 091 387 620 122	−49.457 788 728 082 579 670 330 458 705[a]
1	−46.910 642 653 128 173 651 964 836 840	−48.148 430 420 006 361 035 971 245 463[a]
2	−44.687 033 738 125 528 658 859 863 126	−46.290 753 954 466 087 580 582 890 228
3	−42.042 376 344 470 892 293 963 820 182	−43.968 318 431 814 233 002 577 289 234
4	−39.016 331 198 417 396 568 441 736 596	−41.232 607 772 180 218 479 078 577 843
5	−35.642 628 458 099 764 174 547 675 506	−38.122 785 096 727 919 755 861 765 839
6	−31.952 271 277 351 562 240 663 822 155	−34.672 313 205 699 650 691 489 091 456
7	−27.975 710 623 790 707 492 150 511 028	−30.912 247 487 908 848 263 645 899 252
8	−23.744 764 117 789 411 159 214 855 577	−26.873 448 916 059 872 462 417 069 632
9	−19.294 854 528 177 598 192 875 999 744	−22.588 602 257 693 219 572 212 411 689
10	−14.668 355 694 003 272 192 220 248 503	−18.094 688 282 124 421 158 056 170 233
11	−9.920 787 813 040 383 111 510 031 236	−13.436 869 040 250 076 995 975 578 733
12	−5.135 296 289 270 774 002 472 610 815	−8.676 081 670 736 545 808 091 349 527
13	−0.473 351 957 855 431 951 969 001 641	−3.908 232 481 206 230 174 049 698 348

[a] Reference [40]: $\mathcal{E}_{0,0}=-49.457\,788\,728\,082\,579\,670\,330\,458\,704\,048$, $\mathcal{E}_{1,0}=-48.148\,430\,420\,006\,361\,035\,971\,245\,461\,716$.

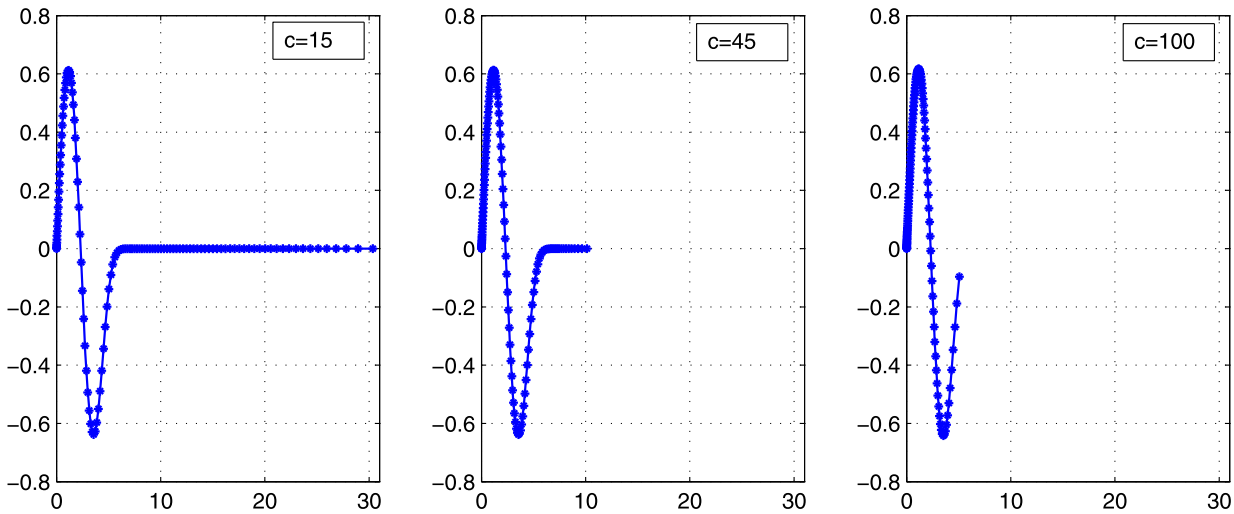

Fig. 2. The first eigenfunction $\Psi_{1,0}(r)=\mathcal{R}_{1,1}^{(1)}(r)$ of the Woods–Saxon potential while c varies.

4. Some remarks on the numerical implementations

A main frame computer is employed for the computations, where the computer code in FORTRAN programming language is executed in quadruple precision arithmetic (30 digits) by truncating the results to 27–28 significant figures. Regardless of which potential function is in question, the diagonalization of an 8×8 matrix with the specified accuracy requires no more than a second whereas it consumes approximately 15 seconds when $N=350$ which is the highest truncation size appearing in our tables.

By the transformation $\xi=(cr)^{\alpha}$ in (6), we have introduced two optimization parameters c and α, which considerably decrease the number of points N used to obtain the desired accuracy. Actually, the first optimization parameter c rescales the points on the half line while the second one α determines the behavior of the eigenfunction at big distances r. When the grid points are collected in the interval where the eigenfunction is nonzero by means of c or the correct behavior of the eigenfunction is caught by the help of α, the desired accuracy can be obtained with the smallest possible truncation order N.

Notice that an eigenfunction of the radial Schrödinger equation is a Gaussian type function. The procedure for choosing the optimum value of c for Gaussian type functions is described in [31]. In short, it is based on the collection of grid points into an interval $(0,K)$ so that none of them are wasted in the interval where the wavefunction is almost zero (see Fig. 2). So the optimum value of c may be determined by the formula $c_{opt}\approx r_N/K$, where r_N is the maximum zero of the $L_{N+1}^{\gamma}(r)$, and K is a point after which the eigenfunction is very close to zero. As a typical example, consider the potential $V(r)=r^2+v_4r^4$, where $v_4>0$. Clearly the required solution will be a function of r^2 (not r!) so that we choose $\alpha=2$ to this end. On the other hand, the selection of the parameter c is closely related to the asymptotic behavior of the solution. To be specific, as $r\to\infty$ the solution behaves like $\exp(-r^2/2)$ when $v_4\ll 1$ and $\exp(-\sqrt{v_4}r^3/3)$ when $v_4>1$, respectively. Since the trial solution we propose in (7) decays like $\exp(-\xi/2)=\exp(-c^2r^2/2)$ in this case where $\alpha=2$, we choose $c=1$

for sufficiently small coupling constants such as $v_4 = 10^{-4}$ (see the first row of Table 1). However, when $v_4 = 10^4$, in order to imitate the true asymptotic behavior $\exp(-100r^3/3)$ of the exact solution, we choose $c = 9$ where we have employed the rule suggested by Tang in [31]. That is, we first observe that $\exp(-100r^3/3) \approx 10^{-20}$ when $r = K \approx 1.1$. On the other hand, the largest zero of the corresponding Laguerre polynomial $L_{30}^{1/2}(\xi)$ is $\xi_N \approx 105.1$ in terms of the transformed variable ξ, or we have $r_N \approx 10.2$ in terms of the original variable r. Therefore, we get $c_{opt} \approx r_N/K \approx 10.2/1.1 \approx 9.3 \approx 9$ (see the ninth row of Table 1).

On the other hand, in general, the optimum value of the second optimization parameter is $0 < \alpha_{opt} \leq 1$. For the lower states of the potentials having countably infinite discrete states besides continuous spectrum, such as ECPSC potential, $\alpha_{opt} = 1$. In contrast, for the higher states of such potentials we have $0 < \alpha_{opt} < 1$ since the first optimization parameter c remains incapable to reflect the correct behavior of the eigenfunction. While $0 < \alpha_{opt} < 1$ we have $c_{opt} = 1$. Therefore, in any case, we do not have to chose two optimization parameters at the same time. Particularly, for the isotropic polynomial potentials in r^2, $\alpha_{opt} = 2$.

5. Conclusion

In this article, we basically employ the Laguerre polynomials $L_n^{\gamma}(\xi)$ satisfying the equation $\xi y'' + (\gamma + 1 - \xi)y' = -ny$, as the trial solutions in (13) and (14) to approximate the solutions of the WPL equation of the form $\xi y'' + (\gamma + 1 - \xi)y' + Q(\xi)y = \lambda \xi^{\frac{2}{\alpha}-1} y$ in a pseudospectral picture, which is an alternative representation of the radial Schrödinger equation in (1). It is important to note that the appropriate γ values in the Laguerre polynomials L_n^{γ} is not selected arbitrarily, but appears naturally in the WPL equation as the parameter $\gamma = (2\ell + M - 2)/\alpha$ in (10).

Recall, in particular, that if $\alpha = 2$ the weight function $\xi^{\frac{2}{\alpha}-1}$ reduces to unity and we may view the WPL equation as the perturbed Laguerre equation, which allows us to cope with the radial Schrödinger equation for potentials $V(r)$ containing only the even powers of r. This type of problems were discussed in our previous article [2] so that just one specific example is presented here, i.e. $V(r) = r^2 + v_4 r^4$ in (53). More generally, the present algorithm with $\alpha \neq 2$ for the WPL equation is now suitable for a larger class of potentials illustrated in Section 3, whose Taylor series expansions contain both even and odd powers of r.

The method is quite general in the sense that many other quantum mechanical eigenvalue problems, for example, with Gaussian, Morse, Deng–Fan, Manning–Rosen and Rosen–Morse potentials, can be handled without any modification. However, we do not include numerical results for these potentials in order not to overfill the content of the paper with tabular material anymore.

References

[1] M. Abramowitz, I.A. Stegun, Handbook of Mathematical Functions with Formulas, Graphs, and Mathematical Tables, Dover, New York, 1970.
[2] H. Alıcı, H. Taşeli, Pseudospectral methods for an equation of hypergeometric type with a perturbation, J. Comput. Appl. Math. 234 (2010) 1140–1152.
[3] P.B. Bailey, B.S. Garbow, H.G. Kaper, A. Zettl, Eigenvalue and eigenfunction computations for Sturm–Liouville problems, ACM Trans. Math. Softw. 17 (1991) 491–499.
[4] P.B. Bailey, W. Everitt, A. Zettl, The SLEIGN2 Sturm–Liouville code, ACM Trans. Math. Softw. 21 (2001) 143–192.
[5] O. Bayrak, I. Boztosun, Bound state solutions of the Hulthén potential by using the asymptotic iteration method, Phys. Scr. 76 (2007) 92–96.
[6] J.P. Boyd, Chebyshev and Fourier Spectral Methods, 2nd ed., Dover Publications Inc., Mineola, NY, 2001.
[7] R.N. Chaudhury, M. Mondal, Eigenvalues of anharmonic oscillators and the perturbed Coulomb problem in N-dimensional space, Phys. Rev. A 52 (1995) 1850–1856.
[8] S. Flügge, Practical Quantum Mechanics, Classics in Mathematics, Springer-Verlag, Berlin, Heidelberg, 1999, reprint of the 1994 edition.
[9] D. Funaro, Polynomial Approximation of Differential Equations, Lecture Notes in Physics, Springer-Verlag, Berlin, Heidelberg, 1992.
[10] B. Gönül, O. Özer, Y. Cançelik, M. Koçak, Hamiltonian hierarchy end the Hulthén potential, Phys. Lett. A 275 (2000) 238–243.
[11] B.Y. Guo, L.L. Wang, Z.Q. Wang, Generalized Laguerre interpolation and pseudospectral method for unbounded domains, SIAM J. Numer. Anal. 43 (6) (2006) 2567–2589.
[12] M. Hamzavi, S.M. Ikhdair, K.E. Thylwe, Equivalence of the empirical shifted Deng–Fan oscillator potential for diatomic molecules, J. Math. Chem. 51 (2013) 227–238.
[13] F.B. Hildebrand, Method of Applied Mathematics, Lecture Notes in Physics, McGraw-Hill, New York, 1956.
[14] L. Hulthén, Ark. Mat. Astron. Fys. A 28 (1942) 5.
[15] S.M. Ikhdair, R. Sever, Approximate ℓ-state solutions of the D-dimensional Schrödinger equation for Manning–Rosen potential, Ann. Phys. 17 (2008) 897–910.
[16] S.M. Ikhdair, R. Sever, Improved analytical approximation to arbitrary ℓ-state solutions of the Schrödinger equation for the hyperbolical potential, Ann. Phys. 18 (2009) 189–197.
[17] L.G. Ixaru, H. De Meyer, G. Vanden Berghe, Highly accurate eigenvalues for the distorted Coulomb potential, Phys. Rev. E 61 (2000) 3151–3159.
[18] C.S. Jia, J.Y. Liu, P.Q. Wang, A new approximation scheme for the centrifugal term and the Hulthén potential, Phys. Lett. A 372 (2008) 4779–4782.
[19] C.S. Lai, Energies of the exponential cosine screened Coulomb potential, Phys. Rev. A 26 (1982) 2245–2248.
[20] V. Ledoux, M. Van Daele, G. Vanden Berghe, CP methods of higher order for Sturm–Liouville and Schrödinger equations, Comput. Phys. Commun. 162 (2004) 151–165.
[21] V. Ledoux, M. Van Daele, G. Vanden Berghe, MATSLISE: a MATLAB package for the numerical solution of Sturm–Liouville and Schrödinger equations, ACM Trans. Math. Softw. 31 (2005) 532–554.
[22] V. Ledoux, M. Van Daele, G. Vanden Berghe, Efficient computation of high index Sturm–Liouville eigenvalues for problems in physics, Comput. Phys. Commun. 180 (2009) 241–250.
[23] J.Q.W. Lo, B.D. Shizgal, Pseudospectral methods of solution of the Schrödinger equation, J. Math. Chem. 44 (2008) 787–801.
[24] G. Mastroianni, D. Occorsio, Lagrange interpolation at Laguerre zeros in some weighted uniform spaces, Acta Math. Hung. 91 (1–2) (2001) 27–52.

[25] K.J. Oyewumi, O.J. Oluwadare, K.D. Sen, O.A. Babalola, Bound state solutions of the Deng–Fan molecular potential with the Pekeris-type approximation using the Nikiforov–Uvarov (N–U) method, J. Math. Chem. 51 (2008) 976–991.
[26] A.K. Roy, The generalized pseudospectral approach to the bound states of the Hulthén and the Yukawa potentials, Pramana J. Phys. 65 (2005) 1–15.
[27] H. Shao, Z. Wang, Arbitrarily precise numerical solutions of the one-dimensional Schrödinger equation, Comput. Phys. Commun. 180 (2009) 1–7.
[28] J. Shen, Stable and efficient spectral methods in unbounded domains using Laguerre functions, SIAM J. Numer. Anal. 38 (2000) 1113–1133.
[29] J. Shen, L.L. Wang, Some recent advances on spectral methods for unbounded domains, Commun. Comput. Phys. 5 (2009) 195–241.
[30] C. Stubbins, Bound states of the Hulthén and the Yukawa potentials, Phys. Rev. A 48 (1993) 220–227.
[31] T. Tang, The Hermite spectral method for Gaussian-type functions, SIAM J. Sci. Comput. 14 (1993) 594–606.
[32] H. Taşeli, An alternative series solution to the isotropic quartic oscillator in N dimensions, J. Math. Chem. 20 (1996) 235–245.
[33] H. Taşeli, Modified Laguerre basis for hydrogen-like systems, Int. J. Quant. Chem. 63 (1997) 949–959.
[34] H. Taşeli, Accurate numerical bounds for the spectral points of the singular Sturm–Liouville problems over $0 < x < \infty$, J. Comput. Appl. Math. 164–165 (2004) 707–722.
[35] H. Taşeli, H. Alıcı, The Laguerre pseudospectral method for the reflection symmetric Hamiltonians on the real line, J. Math. Chem. 41 (2007) 407–416.
[36] H. Taşeli, A. Zafer, Bessel basis with applications: N-dimensional isotropic polynomial oscillators, Int. J. Quant. Chem. 63 (1997) 935–947.
[37] H. Taşeli, A. Zafer, A Fourier–Bessel expansion for solving radial Schrödinger equation in two dimensions, Int. J. Quant. Chem. 61 (1997) 759–768.
[38] L.N. Trefethen, Spectral Methods in MATLAB, SIAM, Philadelphia, 2000.
[39] A. Zafer, H. Taşeli, Two-sided eigenvalue bounds for the spherically symmetric states of the Schrödinger equation, J. Comput. Appl. Math. 95 (1998) 83–100.
[40] A.J. Zakrzewski, Highly precise solutions of the one-dimensional Schrödinger equation with an arbitrary potential, Comput. Phys. Commun. 175 (2006) 397–403.
[41] L.H. Zhang, X.P. Li, C.S. Jia, Approximate solutions of the Schrödinger equation with the generalized Morse potential model including the centrifugal term, Int. J. Quant. Chem. 111 (2012) 1870–1878.